ISSN 2394-3777 (Print)
ISSN 2394-3785 (Online)
Available online at www.ijartet.com

International Journal of Advanced Research Trends in Engineering and Technology (IJARTET)
Vol. 4, Special Issue 11, March 2017

Grid connected hybrid power system

T.Jayapriya[1],A.Gayathri[2],K.Kumar[3],A.Praveena[4],A.Priyanga[5],T.Sowmiya[6].
Department of Electrical and Electronics Engineering,
Idhaya engineering college for women ,chinnasalem,villupuram ,tamilnadu.
Sowmi277@gmail.com[6],aprajag@gmail.com[4],gayu143e@gmail.com[2].

Abstract— In this paper, a control strategy for power flow management of a grid-connected hybrid PV-wind-battery based system with an efficient multi-input transformer coupled bidirectional-dc converter is presented. The proposed system aims to satisfy the load demand, manage the power flow from different sources, inject surplus power into the grid and charge the battery from grid as and when required. A transformer coupled boost half-bridge converter is used to harness power from wind, while bidirectional buck-boost converter is used to harness power from PV along with battery charging/discharging control. A single-phase full-bridge bidirectional converter is used for feeding ac loads and interaction with grid. Here we are increasing the efficiency and reducing ripples and harmonics.the overall control is done by using DSC controller. In addition to this we are having battery back-up to avoid interruption. One single inverter is used to convert AC from wind and solar power.

Keywords— ***Hybrid system, solar photovoltaic, wind energy, transformer coupled boost dual-half-bridge bidirectional converter, bidirectional buck-boost converter, maximum power point tracking, fullbridge bidirectional converter, battery charge control, DSC controller.***

I. INTRODUCTION

In electrical system power failure is more important role in our normal livelihood. Due to supply and demand is not matches in a power system now a days we generate the power without technical knowledge, maintenance, running cost, pollution is better way is solar power generation in our project improve the power reliability to customer with using of PV-battery system. There is different modes of operations are available in this system stage conversion technique is used to improve the efficiency of system and minimize the cost, size, weight. PV systems has been dramatically increased, since, with energy storage, a solar PV system10-2 becomes a stable energy source and it can be dispatched at the request, which results in improving the performance and the value of solar PV systems and wind system. There are different options for integrating energy storage into a utility-scale solar PV system and wind system. Specifically, energy storage can be integrated into the either ac or dc side of the solar PV power conversion systems which may consist of multiple conversion This paper introduces a novel single-stage solar converter called Reconfigurable Solar Converter (RSC). The basic concept of the RSC is to use Using power conversion system to perform different operation modes such as Solar Voltage is healthy and battery is upper low Level and Second one is No solar voltage but Battery is upper low level.

Swift depletion of fossil fuel reserves, ever increasing energy demand and concerns over climate change motivate power generation from renewable energy sources. Solar photovoltaic (PV) and wind have emerged as popular energy sources due to their eco-friendly nature and cost effectiveness. However, these sources are intermittent in nature. Hence, it is a challenge to supply stable and continuous power using these sources. This can be addressed by efficiently integrating with energy storage elements. The interesting complementary behaviour of solar insolation and wind velocity pattern coupled with the above mentioned advantages, has led to the research on their integration resulting in the hybrid PV-wind systems. For achieving the integration of multiple renewable sources, the traditional approach involves using dedicated single-input converters one for each source, which are connected to a common dc-bus. However, these converters are not effectively utilized, due to the intermittent nature of the renewable sources. In addition, there are multiple power conversion stages which reduce the efficiency of the system. Significant amount of literature exists on the integration of solar and wind energy as a hybrid energy generation system with focus mainly on its sizing and optimization . In the sizing of generators in a hybrid system is investigated. In this system, the sources and storage are interfaced at the dc link, through their dedicated converters. Other contributions are made on their modeling aspects and control techniques for a stand-alone hybrid energy system. Dynamic performance of a stand-alone hybrid PV-wind system with battery storage is analyzed. In a passivity/sliding mode control is presented which controls the operation of wind energy system to complement the solar energy generating system. Not many attempts are made to optimize the circuit configuration of these systems that could reduce the cost and increase the efficiency and reliability. In a integrated converters for PV and wind energy systems are

ISSN 2394-3777 (Print)
ISSN 2394-3785 (Online)
Available online at www.ijartet.com
International Journal of Advanced Research Trends in Engineering and Technology (IJARTET)
Vol. 4, Special Issue 11, March 2017

presented. PV-wind hybrid system, has a simple power topology but it is suitable for stand-alone applications. An integrated four-port topology based on hybrid PV-wind system. However, despite simple topology the control scheme used is complex. To feed the dc loads, a low capacity multi-port converter for a hybrid system is presented. Hybrid PV-wind based generation of electricity and its interface with the power grid are the important research areas. Chen et al. in have proposed a multi-input hybrid PV-wind power generation system which has a buck/buck boost fused multi-input dc-dc converter and a full-bridge dc ac inverter. This system is mainly focused on improving the dc-link voltage regulation. In the six-arm converter topology proposed by H. C. Chiang et al. the outputs of a PV array and wind generators are fed to a boost converter to match the dc-bus voltage. The steady-state performance of a grid connected hybrid PV and wind system with battery storage is analyzed . This paper focuses on system engineering, such as energy production, system reliability, unit sizing, and cost analysis. In a hybrid PV-wind system along with a battery is presented, in which both sources are connected to a common dc-bus through individual power converters. In addition, the dc-bus is connected to the utility grid through an inverter. The use of multi-input converter (MIC) for hybrid power systems is attracting increasing attention because of reduced component count, enhanced power density, compactness and centralized control. Due to these advantages, many topologies are proposed and they can be classified into three groups, non-isolated, fully-isolated and partially-isolated multi-port topologies.

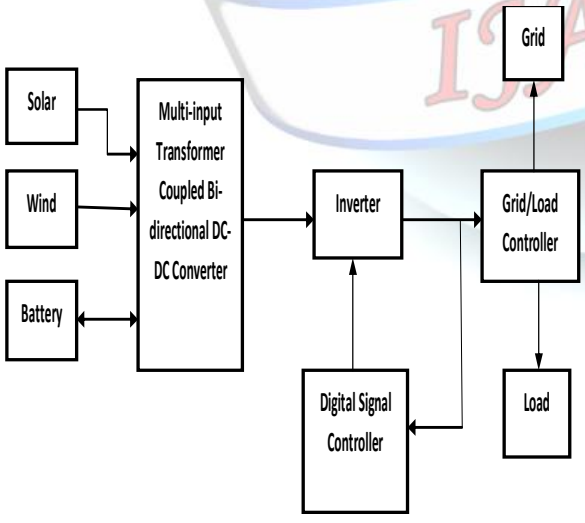

Fig. 1. Grid –connected hybrid PV-wind-battery based system for household applications.

All the power ports in non-isolated multi-port topologies share a common ground. To derive the multi-port dc-dc converters, a series or parallel configuration is employed in the input side. Some components can be shared by each input port. However, a time-sharing control scheme couples each input port, and the flexibility of the energy delivery is limited. The series or parallel configuration can be extended at the output to derive multi-port dc-dc converters. However, the power components cannot be shared. All the topologies in non-isolated multi-port are mostly combinations of basic topology units, such as the buck, the boost, the buck-boost or the bidirectional buck/boost topology unit. These timesharing based multi-port topologies promise low-cost and easy implementation. However, a common limitation is that power from multiple inputs cannot be transferred simultaneously to the load. Further, matching wide voltage ranges will be difficult in these circuits. This made the researchers to prefer isolated multi-port converters compared to non-isolated multi-port dc dc converters. The magnetic coupling approach is used to derive a multiport converter , where the multi-winding transformer is employed to combine each terminal. In fully isolated multiport dc-dc converters, the half-bridge, full-bridge, and hybrid structure based multi-port dc-dc converters with a magnetic coupling solution can be derived for different applications power, voltage, and current levels. The snubber capacitors and transformer leakage inductance are employed to achieve soft switching by adjusting the phase-shift angle. However, the circuit layout is complex and the only sharing component is the multi-winding transformer. So, the disadvantage of time sharing control to couple input port is overcome. Here, among multiple inputs, each input has its own power components which increases the component count. Also, the design of multi-winding transformer is an involved process. In order to address the above limitations, partially isolated multi-port topologies [33] - [39] are becoming increasingly attractive. In these topologies, some power ports share a common ground and these power ports are isolated from the remaining, for matching port voltage levels. A tri-modal half-bridge topology is proposed by Al-Atrash et al. in [33] and [34]. This topology is essentially a modified version of the half-bridge topology with a free-wheeling circuit branch consisting of a diode and a switch across the primary winding of the transformer. The magnetizing inductance of the transformer is used to store energy, and to interface the sources/storage devices. Wuhua Li et.al. [37] - [38], have proposed a decoupled controlled tri-port dc-dc converter for multiple energy interface. The power density is improved and circuit structure is simplified. However, it can interface only one renewable source and energy storage element. Further, the pulse width modulation plus phase-shift control strategy is introduced to provide two control freedoms and achieve the decoupled voltage regulation within a certain

ISSN 2394-3777 (Print)
ISSN 2394-3785 (Online)
Available online at www.ijartet.com
International Journal of Advanced Research Trends in Engineering and Technology (IJARTET)
Vol. 4, Special Issue 11, March 2017

operating range. All the state of the art on converter topologies presented so far can accommodate only one renewable source and one energy storage element. Whereas, the proposed topology is capable of interfacing two renewable sources and an energy storage element. Hence, it is more reliable as two different types of renewable sources like PV and wind are used either individually or simultaneously without increase in the component count compared to the existing state of the art topologies. The proposed system has two renewable power sources, load, grid and battery. Hence, a power flow management system is essential to balance the power flow among all these sources. The main objectives of this system are as follows:

• To explore a multi-objective control scheme for optimal charging of the battery using multiple sources.
• Supplying un-interruptible power to loads.
• Ensuring evacuation of surplus power from renewable sources to the grid, and charging the battery from grid as and when required. The grid-connected hybrid PV-wind-battery based system for household applications is shown in Fig. 1, which can work either in stand-alone or grid connected mode. This system is suitable for household applications, where a low-cost, simple and compact topology capable of autonomous operation is desirable. The core of the proposed system is the multi input transformer coupled bidirectional dc-dc converter that interconnects various power sources and the storage element. Further, a control scheme for effective power flow management to provide uninterrupted power supply to the loads, while injecting excess power into the grid is proposed. Thus, the proposed configuration and control scheme provide an elegant integration of PV and wind energy source.

It has the following advantages:

• MPP tracking of both the sources, battery charging control and bidirectional power flow are accomplished with six controllable switches.
• The voltage boosting capability is accomplished by connecting PV and battery in series which is further enhanced by a high frequency step-up transformer.
• Improved utilization factor of the power converter, since the use of dedicated converters for ensuring MPP operation of both the sources is eliminated.
• Galvanic isolation between input sources and the load.
• The proposed controller can operate in different modes of a grid-connected scheme ensuring proper operating mode selection and smooth transition between different possible operating modes.
• Enhancement in the battery charging efficiency as a single converter is present in the battery charging path from the PV source.

The basic philosophy and preliminary study of a compact and low-cost multi-input transformer coupled dc-dc converter capable of interfacing multiple sources for a stand-alone application is presented . In the present paper, the integration of renewable sources to the grid, detailed analysis, exhaustive simulation and experimental studies have now been included. This paper is organised as follows: In section II, the power circuit configuration of the grid-connected hybrid PV-wind battery system is described along with its analysis. Control strategy for effective power flow management and various operating modes of the system are explained in section III. In sections IV & V, simulation and experimental results are presented to validate the performance of the proposed system. Finally, the conclusions are summarised in section VI.

III EXISTING SYSTEM CONCEPT

In the conventional PV inverter technology, the simple and the low-cost advantage of the flyback topology is promoted only at very low power as micro-inverter .In the applications of inverters, the inverters with five level inversion topology can produce output not as the high step-up output voltage and with high number of switches. Conventional inverter with more number of switches. High power losses. low efficiency. High input current ripple.

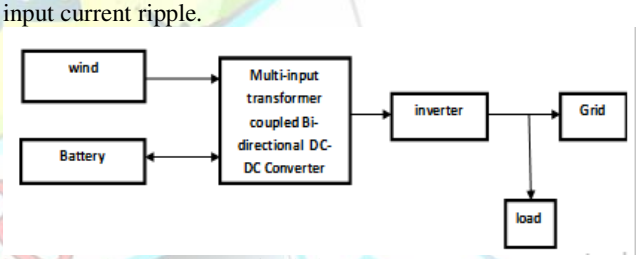

Fig.2. Block diagram of existing system

II *PROPOSED CONVERTER CONFIGURATION*

The proposed converter consists of a transformer coupled boost dual-half-bridge bidirectional converter fused with bidirectional buck-boost converter and a single-phase full-bridge inverter. The proposed converter has reduced number of power conversion stages with less component count and high efficiency compared to the existing grid-connected schemes. The topology is simple and needs only six power switches. The schematic diagram of the converter is depicted in Fig. 2(a). The boost dual-half-bridge converter has two dc-links on both sides of the high frequency transformer. Controlling the voltage of one of the dc-links, ensures controlling the voltage of the other. This makes the control strategy simple. Moreover, additional converters can be integrated with any one of the two dc-links. A bidirectional buck-boost dc-dc converter is integrated with the primary side dc-link and single-phase full bridge bidirectional converter is

ISSN 2394-3777 (Print)
ISSN 2394-3785 (Online)
Available online at www.ijartet.com
International Journal of Advanced Research Trends in Engineering and Technology (IJARTET)
Vol. 4, Special Issue 11, March 2017

connected to the dc-link of the secondary side. The input of the half-bridge converter is formed by connecting the PV array in series with the battery, thereby incorporating an inherent boosting stage for the scheme. The boosting capability is further enhanced by a high frequency step-up transformer. The transformer also ensures galvanic isolation to the load from the sources and the battery. Bidirectional buck boost converter is used to harness power from PV along with battery charging/discharging control. The unique feature of this converter is that MPP tracking, battery charge control and voltage boosting are accomplished through a single converter. Transformer coupled boost half-bridge converter is used for harnessing power from wind and a single-phase full-bridge bidirectional converter is used for feeding ac loads and interaction with grid. The proposed converter has reduced number of power conversion stages with less component count and high efficiency compared to the existing grid-connected converters. We are using dsc ,it is a control the error and protect the system and effective.

DIGITAL SIGNAL CONTROLLER :

- DSC provides both digital signal processing and variety of control operation in single chip.
- DSC provides can provide high speed, low cost , easy to design solution .

Features:

- Fast interrupt handling capability.
- Ability to form address and fetch operands without having bottleneck.
- Hardware to perform MAC operation.

Application:

- DSC used to wide range of application,
- Motor control.
- Power conversion.
- Sensor processing application.
- DSC have fast response.

The power flow from wind source is controlled through a unidirectional boost half-bridge converter. For obtaining MPP effectively, smooth variation in source current is required which can be obtained using an inductor. In the proposed topology, an inductor is placed in series with the wind source which ensures continuous current and thus this inductor current can be used for maintaining MPP current. When switch T 3 is ON, the current flowing through the source inductor increases. The capacitor C1 discharges through the transformer primary and switch T 3 as shown in Fig. 3(b). In secondary side capacitor C3 charges through transformer secondary and anti-parallel diode of switch T 5. When switch T 3 is turned OFF and T 4 is turned ON, initially the inductor current flows through antiparallel diode of switch T 4 and through the capacitor bank. The path of current is shown in Fig. 3(c). During this interval, the current flowing through diode decreases and that flowing through transformer primary increases. When current flowing through the inductor becomes equal to that flowing through transformer primary, the diode turns OFF. Since, T 4 is gated ON during this time, the capacitor C2 now discharges through switch T 4 and transformer primary. During the ON time of T 4, anti-parallel diode of switch T 6 conducts to charge the capacitor C4. The path of current flow is shown in Fig. 2(d). During the ON time of T 3, the primary voltage $V_P = -V_{C1}$. The secondary voltage $V_S = nV_p = -nV_{C1} = -V_{C3}$, or $V_{C3} = nV_{C1}$ and voltage across primary inductor L_w is V_w. When T 3 is turned OFF and T 4 turned ON, the primary voltage $V_P = V_{C2}$. Secondary voltage $V_S = nV_P = nV_{C2} = V_{C4}$ and voltage across primary inductor L_w is $V_w - (V_{C1} + V_{C2})$. It can be proved that $(V_{C1} + V_{C2}) = \frac{V_w}{(1-D_w)}$. The capacitor voltages are considered constant in steady state and they settle at $V_{C3} = nV_{C1}$, $V_{C4} = nV_{C2}$. Hence the output voltage is given by

$$V_{dc} = V_{C3} + V_{C4} = n \frac{V_w}{(1 - D_w)} \quad (1)$$

Therefore, the output voltage of the secondary side dc-link is a function of the duty cycle of the primary side converter and turns ratio of transformer. In the proposed configuration as shown in Fig. 2(a), a bidirectional buck-boost converter is used for MPP tracking of PV array and battery charging/discharging control. Further, this bidirectional buck-boost converter charges/discharges the capacitor bank C1-C2 of transformer coupled half-bridge boost converter based on the load demand. The half-bridge boost converter extracts energy from the wind source to the capacitor bank C1-C2. During battery charging mode, When switch T 1 is ON, the energy is stored in the inductor L. When switch T 1 is turned OFF and T 2 is turned ON, energy stored in L is transferred to the battery. If the battery discharging current is more than the PV current, inductor current becomes negative.

ISSN 2394-3777 (Print)
ISSN 2394-3785 (Online)
Available online at www.ijartet.com

International Journal of Advanced Research Trends in Engineering and Technology (IJARTET)
Vol. 4, Special Issue 11, March 2017

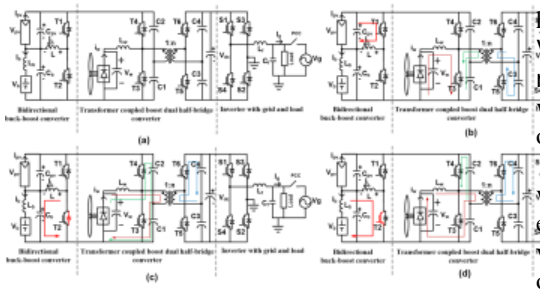

Fig . 3. Operating modes of proposed multi-input transformer coupled bidirectional dc-dc converter. (a) Proposed converter configuration. (b) Operation when switch T3 is turned ON. (c) Operation when switch T4 ON, charging the capacitor bank. (d) Operation when switch T4 ON, capacitor C2 discharging.

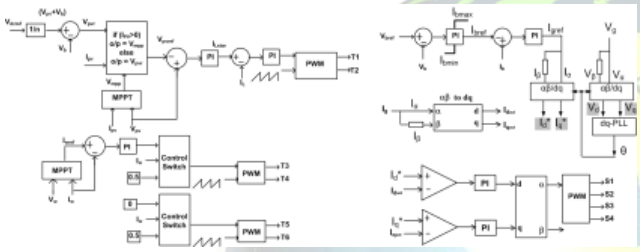

Fig. 4. Proposed control scheme for power flow management of a grid-connected hybrid PV-wind-battery based system.

Here, the stored energy in the inductor increases when T_2 is turned on and decreases when T_1 is turned on. It can be proved that $V_b = \frac{D}{1-D} V_{pv}$. The output voltage of the transformer coupled boost half-bridge converter is given by,

$$V_{dc} = n(V_{C1} + V_{C2}) = n(V_b + V_{pv}) = n \frac{V_w}{(1 - D_w)} \quad (2)$$

This voltage is n times of primary side dc-link voltage. The primary side dc-link voltage can be controlled by half-bridge boost converter or by bidirectional buck-boost converter. The relationship between the average value of inductor, PV and battery current over a switching cycle is given by $I_L = I_b + I_{pv}$. It is evident that, I_b and I_{pv} can be controlled by controlling I_L. Therefore, the MPP operation is assured by controlling I_L while maintaining proper battery charge level. I_L is used as inner loop control parameter for faster dynamic response while for outer loop, capacitor voltage across PV source is used for ensuring MPP voltage. An incremental conductance method is used for MPPT.

A. Limitations and Design issues

The output voltage V_{dc} of transformer coupled boost dual half-bridge converter, depends on MPP voltage of PV array V_{PV_mpp}, the battery voltage V_b and the transformer turns ratio n. Since the environmental conditions influence PV array voltage and the battery voltage depends on its charge level, the output dc-link voltage V_{dc} is also influenced by the same.

However, the PV array voltage exhibits narrow variation in voltage range with wide variation in environmental conditions. On the other hand, the battery voltage is generally stiff and it remains within a limited range over its entire charge-discharge cycle. Further, the SOC limits the operating range of the batteries used in a stand-alone scheme to avoid overcharge or discharge. Therefore, with proper selection of n, PV array and battery voltage the output dc-link voltage V_{dc} can be kept within an allowable range, though not controllable. However, when there is no PV power, by controlling the PV capacitor voltage the output dc-link voltage V_{dc} can be controlled.

III. Proposed Control Scheme for Power Flow Management

A grid-connected hybrid PV-wind-battery based system consisting of four power sources (grid, PV, wind source and battery) and three power sinks (grid, battery and load), requires a control scheme for power flow management to balance the power flow among these sources. The control philosophy for power flow management of the multi-source system is developed based on the power balance principle. In the stand-alone case, PV and wind source generate their corresponding MPP power and load takes the required power. In this case, the power balance is achieved by charging the battery until it reaches its maximum charging current limit I_{bmax}. Upon reaching this limit, to ensure power balance, one of the sources or both have to deviate from their MPP power based on the load demand. In the grid-connected system both the sources always operate at their MPP. In the absence of both the sources, the power is drawn from the grid to charge the battery as and when required. The equation for the power balance of the system is given by:

$$V_{PV} I_{PV} - V_W I_W = V_b I_b + V_g I_g \quad (3)$$

The peak value of the output voltage for single phase full-bridge inverter is,

$$\hat{V} = m_a V_{dc} \quad (4)$$

And the dc-link voltage is,

$$V_{dc} = n(V_{pv} + V_b) \quad (5)$$

Hence, by substituting for V_{dc} in (4), given,

ISSN 2394-3777 (Print)
ISSN 2394-3785 (Online)
Available online at www.ijartet.com
International Journal of Advanced Research Trends in Engineering and Technology (IJARTET)
Vol. 4, Special Issue 11, March 2017

$$V_g - \frac{1}{\sqrt{2}} m_a n (V_{PV} + V_b) \quad (6)$$

In the boost half-bridge converter,

$$V_w = (1 - D_w)(V_{PV} + V_b) \quad (7)$$

Now substituting V_w and V_g in (3)

$$V_{PV} I_{PV} + (V_{PV} + V_b)(1 - D_w) I_w = V_b I_b + \frac{1}{\sqrt{2}} m_a n (V_{PV} + V_b) I_g \quad (8)$$

After simplification,

$$I_b = I_{PV} \left(\frac{1 - D_{PV}}{D_{PV}} \right) + I_W \left(\frac{1 - D_W}{D_{PV}} \right) - I_g \left(\frac{m_a n}{\sqrt{2} D_{PV}} \right) \quad (9)$$

TABLE I. SIMULATION PARAMETERS

Parameter	Value
Solar PV power	525 W (I_{mpp} = 14.8 A) (V_{mpp} = 35.4 V)
Wind power	300 W (I_{mpp} = 8 A) (V_{mpp} = 37.5 V)
Switching frequency	15 kHz
Transformer turns ratio	5.5
Inductor-half bridge boost converter, L_w	500 μH
Inductor-bidirectional converter L	3000 μH
Primary side capacitors C1-C2	500μF
secondary side capacitors C3-C4	500μF
Secondary side capacitor for the entire dc-link	2000 μF
Battery capacity & voltage	400 Ah, 36 V

From the above equation it is evident that, if there is a change in power extracted from either PV or wind source, the battery current can be regulated by controlling the grid current I_g. Hence, the control of a single-phase full-bridge bidirectional converter depends on availability of grid, power from PV and wind sources and battery charge status. Its control strategy is illustrated using Fig. 3. To ensure the supply of uninterrupted power to critical loads, priority is given to charge the batteries. After reaching the maximum battery charging current limit the surplus power from renewable sources is fed to the grid. In the absence of these sources, battery is charged from the grid.

II. SIMULATION RESULTS AND DISCUSSION

Detailed simulation studies are carried out on MATLAB/ Simulink platform and the results obtained for various operating conditions are presented in this section. Values of parameters used in the model for simulation are listed in Table I.

The steady state response of the system during the MPPT mode of operation is shown in Fig. 4. The values for source-1 (PV source) is set at 35.4 V (V_{mpp}) and 14.8 A (I_{mppp}), and for source-2 (wind source) is set at 37.5 V (V_{mpp}) and 8 A (I_{mppp}). It can be seen that V_{pv} and I_{pv} of source-1, and V_w and I_w of source-2 attain set values required for MPP operation. The battery is charged with the constant magnitude of current and remaining power is fed to the grid.

The system response for step changes in the source-1 insolation level while operating in MPPT mode is shown in Fig. 5. Until 2 s, both the sources are operating at MPPT and charging the battery with constant current and the remaining power is fed to the grid. At instant 2 s, the source-1 insolation level is increased. As a result the source-1 power increases and both the sources continue to operate at MPPT. Though the source-1 power has increased, the battery is still charged with the same magnitude of current and power balance is achieved by increasing the power supplied to the grid. At instant 4 s, insolation of source-1 is brought to the same level as before 2s. The power supplied by source-1 decreases. Battery continues to get charged at the same magnitude of current, and power injected into the grid decreases. The same results are obtained for step changes in source-2 wind speed level. These results

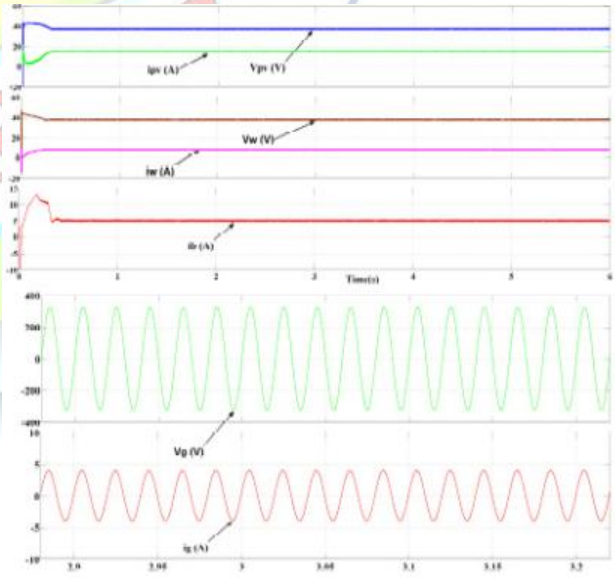

Fig.5. Steady state operation in MPPT mode.

ISSN 2394-3777 (Print)
ISSN 2394-3785 (Online)
Available online at www.ijartet.com

International Journal of Advanced Research Trends in Engineering and Technology (IJARTET)
Vol. 4, Special Issue 11, March 2017

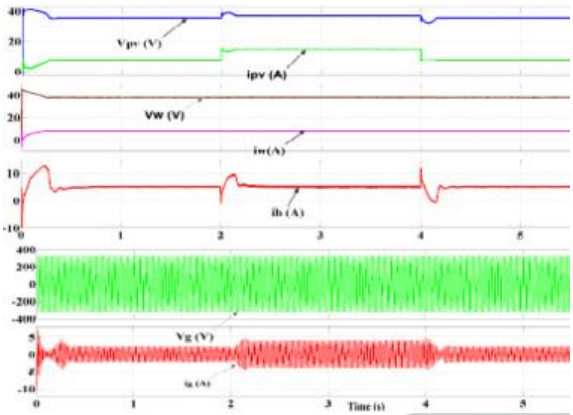

Fig.6. Response of the system for changes in isolation level of source-1 (PV source) during operation in MPPT mode.

are shown in Fig. 7.

The response of the system in the absence of source-1 is shown in Fig. 8. Till time 2 s, both the sources are generating the power by operating at their corresponding MPPT and charging the battery at constant magnitude of current, and the remaining power is being fed to the grid. At 2 s, source- 1 is disconnected from the system. The charging current of the battery remains constant, while the injected power to the grid reduces. At instant 4 s, source-1 is brought back into the system. There is no change in the charging rate of the battery.The additional power is fed to grid. The same results are obtained in the absence of source-2. These results are shown in Fig. 9. Fig. 10shows the results in the absence of both PV and wind power, battery is charged from the grid.

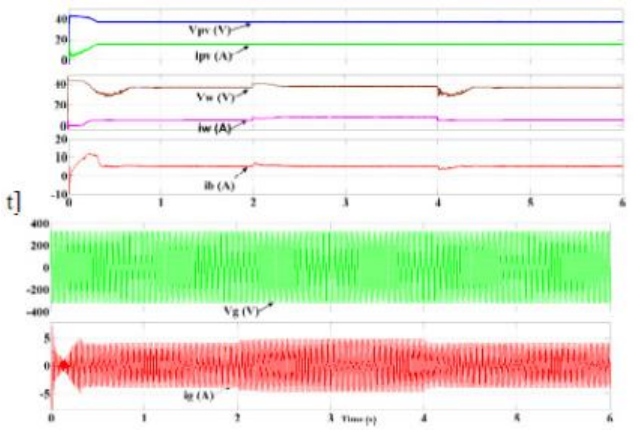

Fig.7. Response of the system for changes in isolation level of source-2 (wind source) during operation in MPPT mode.

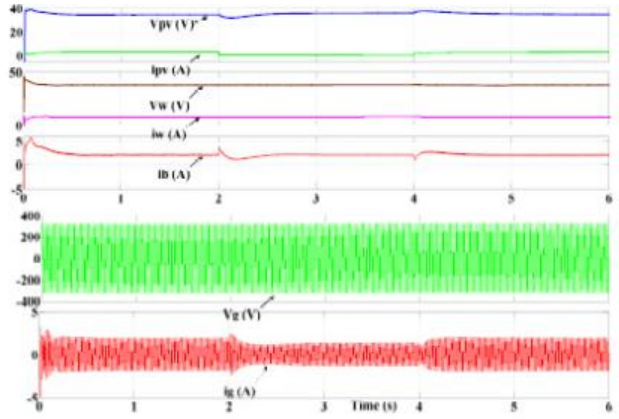

Fig.8. Response of the system in the absence of source-1 (PV source) while source-2 continues to operate at MPPT.

III. EXPERIMENTAL VALIDATION

To verify the simulation results, experimental tests are carried out on a laboratory prototype shown in Fig. 10. The specifications of experimental set up are given in Table II. The control strategy is implemented by employing Texas Instruments floating-point DSP, TMS320F28335. [5] presented a brief outline on Electronic Devices and Circuits which forms the basis of the Clampers and Diodes.

A. Design of multi-input transformer coupled dc-dc converter

The MPP voltage of the PV is considered as 36 V (V_{mpp}). The nominal voltage level of the battery is chosen as 36 V (V_b). The voltage across the dc-bus at the primary side of the transformer is ($V_{c1} + V_{c2}$) which is equal to ($V_{pv}+V_b$). It implies that this dc-bus voltage depends on the magnitude of V_{pv} and V_b. An overall variation of ± 10 V on ($V_{pv}+V_b$) is considered for design purpose and thus overall variation in this dc-bus is in the range of 62-82 V.

The dc-bus voltage at the transformer secondary side, V_{dc} is

ISSN 2394-3777 (Print)
ISSN 2394-3785 (Online)
Available online at www.ijartet.com

International Journal of Advanced Research Trends in Engineering and Technology (IJARTET)
Vol. 4, Special Issue 11, March 2017

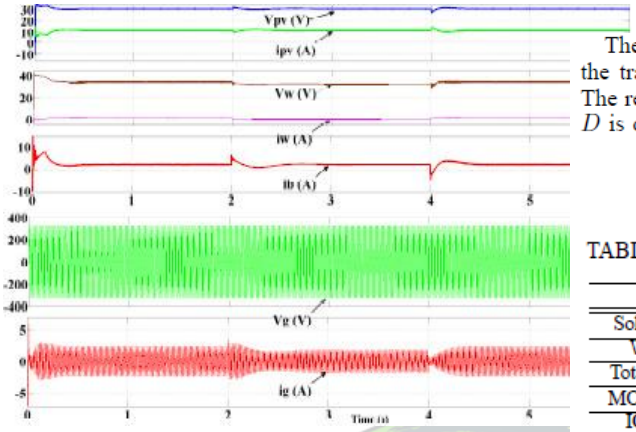

Fig.9. Response of the system in the absence of source-2 (wind source) while source -1 continues to operate at MPPT.

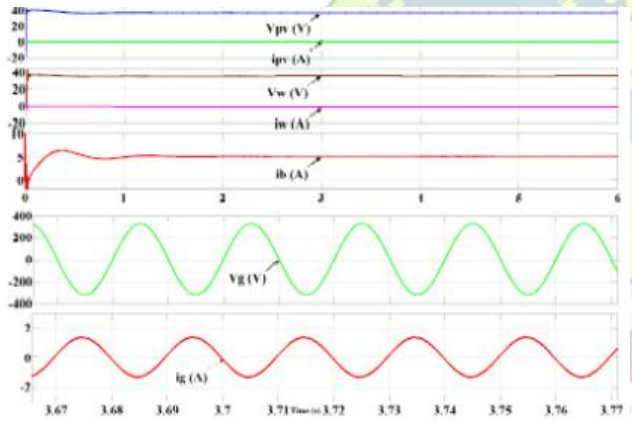

Fig.10. Response of the system in the absence of both the source and charging the battery from grid.

required to be maintained at 350 V. Since, the dc-link voltage at secondary side is 'n times the dc-link voltage at primary side, 'n turns out to be 5.65 (=350/62). Now, considering voltage drops at transformer primary and secondary sides, the turns ratio is chosen to be 6. During ON/OFF operation of switches T3 and T4 (Fig.2), each of the capacitors, C1 and C2, appear across the transformer primary winding. Considering the range of variation of voltage of the wind source as 36-44 V, the capacitors C1 and C2 will experience a voltage in the range of 18-46 V (calculation is given below). Therefore, by keeping a small safety factor, the transformer primary voltage is chosen as 50 V. Thus, the secondary voltage rating is chosen as, 6 × 50 V = 300 V. The transformer chosen has a capacity of 1kVA.

The range for V_w=36-44 V, and the range for the dc-bus on the transformer primary side, V_{bus} (Vc1 + Vc2) is 62-82 V. The relationship between V_w and V_{bus} is, $V_{bus} = \frac{V_w}{1-D}$, where D is duty ratio of switch T3. For V_w=44 V, and V_{bus} = 82 V,

$$D = 1 - \left(\frac{V_w}{V_{bus}}\right) = 0.46. \quad (10)$$

TABLE II. SPECIFICATIONS OF EXPERIMENTAL SET UP

Parameter	Value	Part number
Solar PV power	250 W	
Wind power	250 W	
Total load power	500 W	
MOSFET- T1-T4	200 V, 90 A	IRFP4668PbF
IGBT- S1-S4	1200 V, 20 A	IRG7PH35UD1PbF
Diode- D1-D2	1000 V,60 A	STTH6010W
Capacitor- C_b	1000μF, 100 V	SLPX102M100A3P3
Capacitor- C1-C2	560μF, 100 V	100ZLJ560M
Capacitor- C3-C4	560μF, 400 V	MCLPR400V567M
Capacitor- C_w	1000μF, 63 V	ECA1JHG102
Capacitor- C_{pv}	2000μF, 200 V	CGS202T200V4C
Inductor- L	3000μH, 40 A	
Inductor -L_w	500μH, 50 A	
Inductor -L_b	1000μH, 30 A	
Battery	12 X 3 V, 7.2 Ah	

In steady state,

$$DVc1 - (1 - D)Vc2 = 0, \quad (11)$$

and $Vc1 + Vc2 = V_{bus}$. From these equations, various values for $Vc1$ and $Vc2$ considering all extreme cases are given in Table III.

TABLE III. RANGES OF V_{c1} AND V_{c2} FOR VALUES OF V_w AND V_{bus}

V_w (V)	V_{bus} (V)	D	$1-D$	V_{c1} (V)	V_{c2} (V)
44	82	0.46	0.53	44	38
36	82	0.56	0.44	36	46
44	62	0.29	0.71	44	18
36	62	0.42	0.58	36	26

The steady state response of the system during the MPPT mode of operation is shown in Fig. 11. The values for source-1 (PV source) and source-2 (wind source), are set at 40 V (V_{mpp}) and 5 A (I_{mppp}) respectively and both the sources attain the set value required for MPP operation. The battery is charged at a constant magnitude of current and remaining power is fed to the grid.

The system response for step changes in the source-1 insolation level while operating in MPPT mode is shown in Fig. 12. Until time t1, both the sources are operating at MPPT, battery is charged at a constant current and the remaining power is fed to the grid. At time t1, source-1 insolation level is increased. As a result the source-1 power increases. Both

ISSN 2394-3777 (Print)
ISSN 2394-3785 (Online)
Available online at www.ijartet.com

International Journal of Advanced Research Trends in Engineering and Technology (IJARTET)
Vol. 4, Special Issue 11, March 2017

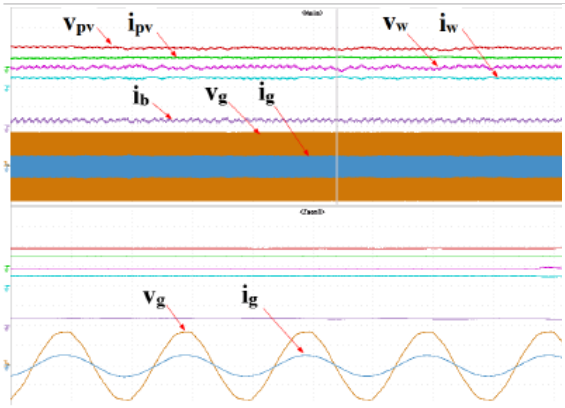

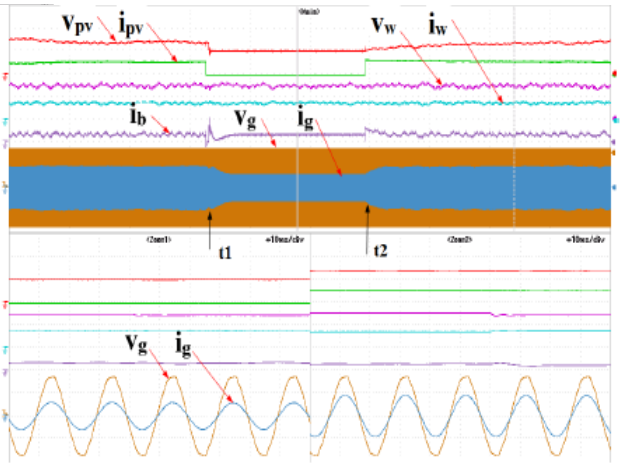

Fig.11. steady state operation in MPPT mode (V_{PV}=10V/div); I_{PV}=2A/div;V_W=20V/div;I_W=2A/div; V_g=200V/div; I_g=2A/div ; I_b=2A/div;` Zoomed version of V_g & I_g during steady state operation.

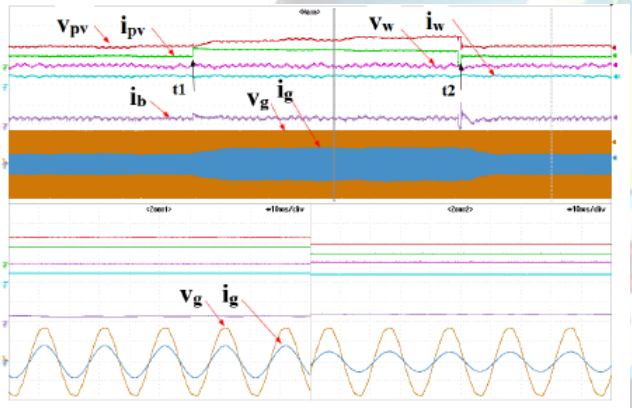

Fig.12. Response of the system for changes in isolation level of source -1(PV source) during operation in MPPT mode (V_{PV}=10V/div;I_{PV}=1A/div;V_W=50V/div;I_W=5A/div; V_g=200V/div; I_g=2A/div ; I_b=2A/div;` Zoomed version of V_n & I_n during steady state operation.

Fig.13. Response of the system in the absence of source -1 (PV source) source-2 (wind source) continues to operate at MPPT mode (V_{PV}=10V/div);I_{PV}=1A/div;V_W=50V/div;I_W=5A/div; V_g=200V/div; I_g=2A/div ; I_b=2A/div; Zoomed version of V_g & I_g during steady state operation.

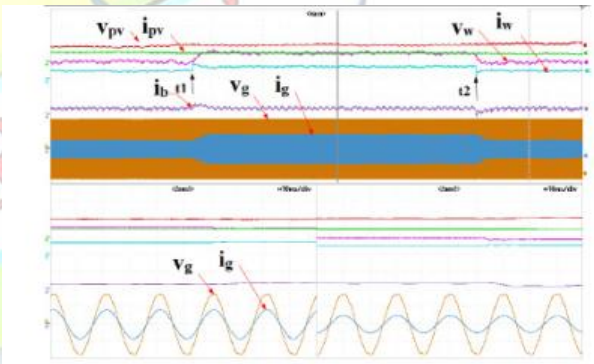

Fig. 14. Response of the system for changes in wind speed level of source-2 (wind source) during operation in MPPT mode (v_{pv}=10V/div; i_{pv}=1A/div; v_w=10V/div; i_w=1A/div; v_g=200V/div; i_g=2A/div; i_b=2A/div). Zoomed version of v_g & i_g during step change in insolation.

ISSN 2394-3777 (Print)
ISSN 2394-3785 (Online)
Available online at www.ijartet.com

International Journal of Advanced Research Trends in Engineering and Technology (IJARTET)
Vol. 4, Special Issue 11, March 2017

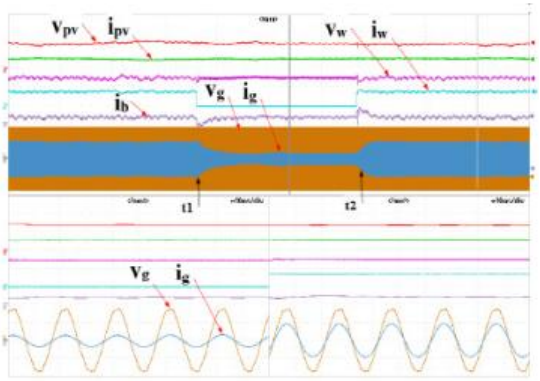

Fig. 15. Response of the system in the absence of source-2 (wind sourc while source-1 continues to operate at MPPT (v_{pv}=10V/div; i_{pv}=1A/di v_w=10V/div; i_w=1A/div; v_g=200V/div; i_g=2A/div; i_b=2A/div). Zoomed ve sion of v_g & i_g in the absence of source-2.

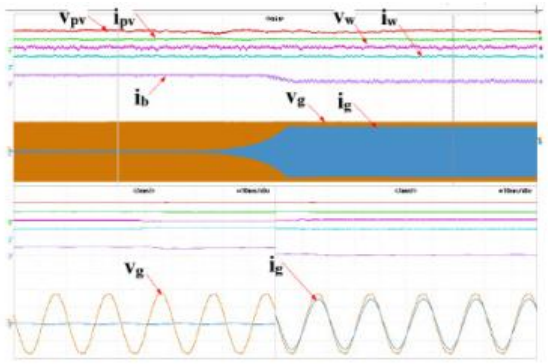

Fig. 16. Response of the system during changes of the operating mode from grid-connected without injection to grid-connected with injection (v_{pv}=10V/div; i_{pv}=1A/div; v_w=10V/div; i_w=1A/div; v_g=200V/div; i_g=2A/div; i_b=2A/div). Zoomed version of v_g & i_g during mode transition.

The sources continue to operate at MPP. Though the source-1 power has increased, the battery is still charged at the same
magnitude of current. The additional power is fed to the grid. At time t2, source-1 is brought to the same insolation level as before t1. The power generated by the source-1 decreases, and there is no change in charging current of the battery. The power injected to the grid decreases. The same results are obtained for step changes in source-2 wind speed level. These results are shown in Fig. 14.

The response of the system without source-1 is shown in Fig. 13. Till time t1, both the sources are present in the system, operating at their corresponding MPP and charging the battery at constant magnitude of current. The remaining power is fed to the grid. At time t1, source-1 is disconnected from the system. However, the battery continues to get charged at the same rate, and the power injected into the grid reduces. At time t2, source- 1 is brought back into the system. This additional power is injected into the grid. The same results are obtained in the absence of source-2. These results are shown in Fig. 15.

Fig. 16 shows that when the battery reaches its float voltage V_{bref}, it goes to constant voltage mode. The surplus power from the renewable sources is fed to the grid. It is clear that before the battery reaches its float voltage the current injected into grid is zero, and it increases thereafter.

IV. CONCLUSION

Hybrid PV-wind – battery based power evacuation scheme for household application is proposed. The proposed hybrid system provides an elegant integration of PV and wind source to extract maximum energy from the to source .it is realized by a novel multi-input transformer coupled bi-directional dc-dc converter followed by a conventional full-bridge inverter .when less power or errors occurs from inverter, to rectify it we use DSC between inverter and grid .DSC is the best controller when compare to other controller in this system. Detailed simulation studies are carried out to ascertain the viability of the scheme. The experimental results obtained are in close agreement with simulations and supportive in demonstrating the capability of the system to operate either in grid feeding or stand –alone mode .the proposed configuration is capable of supplying un – interruptible power to ac loads ,and ensures evacuation surplus PV and Wind power in to grid.

REFERENCES

[1] F. Valenciaga and P. F. Puleston, "Supervisor control for a stand-alone hybrid generation system using wind and photovoltaic energy," *IEEE Trans. Energy Convers.,* vol. 20, no. 2, pp. 398-405, Jun. 2005.

[2] C. Liu, K. T. Chau and X. Zhang,"An efficient wind-photovoltaic hybrid generation system using doubly excited permanent-magnet brushless machine,"*IEEE Trans. Ind. Electron.,* vol. 57, no. 3, pp. 831-839, Mar. 2010.

[3] W. Qi, J. Liu, X. Chen, and P. D. Chris to fides, "Supervisory predictive control of standalone wind/solar energy generation systems," *IEEE*

ISSN 2394-3777 (Print)
ISSN 2394-3785 (Online)
Available online at www.ijartet.com

International Journal of Advanced Research Trends in Engineering and Technology (IJARTET)
Vol. 4, Special Issue 11, March 2017

Trans. Control Sys. Tech., vol. 19, no. 1, pp. 199-207, Jan. 2011.

[4] F. Giraud and Z. M. Salameh, "Steady-state performance of a grid connected rooftop hybrid wind-photovoltaic power system with battery storage," *IEEE Trans. Energy Convers.,* vol. 16, no. 1, pp. 1-7, Mar. 2001.

[5] Christo Ananth, W.Stalin Jacob, P.Jenifer Darling Rosita. "A Brief Outline On ELECTRONIC DEVICES & CIRCUITS.", ACES Publishers, Tirunelveli, India, ISBN: 978-81-910-747-7-2, Volume 3,April 2016, pp:1-300.

[6] M. Dali, J. Belhadj and X. Roboam, "Hybrid solar-wind system with battery storage operating in grid-connected and standalone mode: control and energy management-experimental investigation," *Energy,* vol. 35, no. 6, pp. 2587-2595, June 2010.

[7] W. Kellogg, M. Nehrir, G. Venkataramanan, and V. Gerez, "Generation unit sizing and cost analysis for stand-alone wind, photovoltaic and hybrid wind/PV systems, "*IEEE Trans. Ind. Electron.,* vol. 13, no. 1, pp. 70-75, Mar. 1998.

[8] L. Xu, X. Ruan, C. Mao, B. Zhang, and Y. Luo,"An improved optimal sizing method for wind-solar-battery hybrid power system," *IEEE Trans. Sustainable Enery.,* vol. 4, no. 3, pp. 774785, Jul. 2013.

[9] B. S. Borowy and Z. M. Salameh,"Dynamic response of a stand-alone wind energy conversion system with battery energy storage to a wind gust,"*IEEE Trans. Energy Convers.,* vol. 12, no. 1, pp. 73-78, Mar. 1997.

[10] S. Bae and A. Kwasinski,"Dynamic modeling and operation strategy for a microgrid with wind and photovoltaic resources," *IEEE Trans. Smart Grid,* vol. 3, no. 4, pp. 1867-1876, Dec. 2012.

[11] C. W. Chen, C. Y. Liao, K. H. Chen and Y. M. Chen,"Modeling and controller design of a semi isolated multi input converter for a hybrid PV/wind power charger system," *IEEE Trans. Power Electron.,* vol. 30, no. 9, pp. 4843-4853, Sept. 2015.

[12] M. H. Nehrir, B. J. LaMeres, G. Venkataramanan, V. Gerez, and L. A. Alvarado, "An approach to evaluate the general performance of stand-alone wind/photovoltaic generating systems, "*IEEE Trans. Energy Convers.,* vol. 15, no. 4, pp. 433-439, Dec. 2000.

[13] W. M. Lin, C. M. Hong, and C. H. Chen, "Neural network-based MPPT control of a stand-alone hybrid power generation system," *IEEE Trans. Power Electron.,* vol. 26, no. 12, pp. 3571-3581, Dec. 2011.

[14] F. Valenciaga, P. F. Puleston, and P. E. Battaiotto ,"Power control of a solar/wind generation system without wind measurement: a passivity/ sliding mode approach, "*IEEE Trans. Energy Convers.,* vol. 18, no. 4, pp. 501-507, Dec. 2003.

[15] T. Hirose and H. Matsuo, "Standalone hybrid wind-solar power generation system applying dump power control without dump load," *IEEE Trans. Ind. Electron.,* vol. 59, no. 2, pp. 988-997, Feb. 2012.